EXPLORING PATTERNS IN MICROPLASTIC POLLUTION IN A LARGE RURAL WATERSHED

by

EMILY MARTIN

(Under the Direction of Krista Capps and Stephen Golladay)

ABSTRACT

Microplastics are a ubiquitous contaminant of emerging concern and their movement through freshwater systems is an understudied part of the "plastic cycle." To assess spatial and temporal variation in the composition and concentration of microplastics in a river system, I collected monthly surface water samples from 16 sites in an agriculturally dominated watershed in southwestern Georgia. I used generalized linear models (GLMMs) to investigate relationships among plastics, land use variables, and physicochemical properties. The analyses suggested that microplastic concentrations are strongly related to soluble reactive phosphorous (SRP) in the water column. These findings enhance our understanding of plastic pollution dynamics in rural watersheds.

INDEX WORDS: Plastic Pollution, Microplastics, Freshwater, Water Quality

EXPLORING PATTERNS IN MICROPLASTIC POLLUTION IN A LARGE RURAL WATERSHED

by

EMILY MARTIN

Bachelor of Science, State University of New York at Geneseo, 2018

A Thesis Submitted to the Graduate Faculty of The University of Georgia in Partial Fulfillment of the Requirements for the Degree

MASTER OF SCIENCE

ATHENS, GEORGIA

2022

EXPLORING PATTERNS IN MICROPLASTIC POLLUTION IN A LARGE RURAL WATERSHED

by

EMILY MARTIN

Major Professors:	Krista Capps
	Stephen Golladay
Committee:	Rae McNeish

Electronic Version Approved:

Ron Walcott
Vice Provost for Graduate Education and Dean of the Graduate School
The University of Georgia
December 2022

DEDICATION

I dedicate this work to my grandparents, John and Patricia, for instilling in me a love for the outdoors and a fascination with natural systems. Thank you for allowing me to play in the swamp as a child and encouraging me to continue doing so as an adult. I wouldn't be here without you.

ACKNOWLEDGEMENTS

I want to thank my advisors, Krista Capps and Stephen Golladay, and my committee member, Rae McNeish, for guiding me through my program and pushing me to be a better scientist. Thanks to the Odum School of Ecology, the Jones Center at Ichauway, and the Savannah River Ecology Lab for funding this project. Special thanks to Maddie Monroe, my lab mate and friend, who helped me every step of the way. Caitlin Sweeney helped with field sampling, processing water quality samples, and data management. Bryan Cloninger analyzed nutrient samples and provided logistical support. Jean Brock assisted with GIS. Maxine Hauser and Jamie Rogers helped me with lab prep. Kiersten Nelson, Chloe Eggert, George Jenson, McKayla Susen, Chris Smaga, Corinne Sweeney, and Ben Webster offered friendship and advice. Thank you to my family and my partner, Uriaha, for their love and encouragement. Especially my mom, Gina. I love you.

TABLE OF CONTENTS

Page

LIST OF TABLES

Page

LIST OF FIGURES

Page

CHAPTER 1

INTRODUCTION

Microplastics are a contaminant of emerging concern pervasive in terrestrial and aquatic ecosystems worldwide (Rochman et al. 2019, Hoellein et al. 2019, Li et al. 2020). Due to their microscopic size (<5 mm), diversity, and resistance to degradation (Geyer et al. 2017), microplastics' ubiquity in natural environments has sparked concern about the potential effects on human health and ecosystem function, particularly in aquatic systems. Microplastic pollution presents various toxicological risks to human health (Vethaak and Legler 2021). Additionally, research has shown that microplastics can concentrate pollutants, move through food webs, and affect microbial communities (McCormick et al. 2014, Wright and Kelly 2017). Recent projections of global plastic production and consumption indicate that emissions into aquatic environments will continue to increase unless the global plastic economy experiences drastic change (Borrelle 2020). However, our understanding of how microplastics cycle within and move throughout ecosystems is still limited, especially in freshwater systems (Hoellein and Rochman 2021).

Early microplastic research focused on marine and coastal environments and assumed that rivers acted as conduits for transporting plastic directly from terrestrial to marine systems, neglecting to consider patterns in retention or resuspension within watersheds (Hoellein et al. 2019, Rillig 2020). This is unsurprising as the diversity of sources and forms of microplastic pollution make it difficult to estimate inputs to freshwater environments (Rochman et al. 2019). Recently, a framework of the "plastic cycle" has been proposed for terrestrial and freshwater

systems that conceptually demonstrates how plastics travel through and interact with the environment (Hoellein and Rochman 2021). Hoellein & Rochman (2021) argue that scientists should consider modeling plastics as an element possessing a unique biogeochemical cycle. To support this type of approach, additional empirical data are needed to generate a comprehensive understanding of microplastic sources, sinks, and fluxes in freshwater systems.

Due to the heterogeneous distribution of microplastic contamination and poor understanding of non-point sources, watershed-scale approaches to modeling plastic may better allow scientists to elucidate the driving factors behind microplastic fluxes in riverine systems (Barrows et al., 2018). Due to the anthropogenic nature of plastic pollution, most studies have been conducted in urban watersheds. Relatively less attention has been directed toward understanding plastic dynamics in rural watersheds, presenting a knowledge gap in how microplastics are accumulated and exported in a diversity of settings (Eibes and Gabel 2022). This information is critical for estimating microplastic loads and fluxes in a broader context. For example, plastic pollution in watersheds dominated by agriculture may experience increased topsoil loading of microplastics due to practices such as biosolid application, plasticulture, and composting (Brandes et al. 2021). As a result, agricultural fields susceptible to topsoil erosion could be a considerable source of microplastic pollution in aquatic systems (Rehm et al. 2021).

Research suggests that microplastic, an allochthonous form of carbon, behaves similarly to naturally occurring particles relative to transport, deposition, and breakdown patterns in riverine systems (Kumar et al. 2021, Yan et al. 2021). For instance, microplastic has been shown to follow depositional patterns of natural particles in rivers in experimental settings (Khatmullina and Isachenko 2017, Waldschläger and Schüttrumpf 2019, Hoellein et al. 2019). However, there is little empirical evidence available on the relationship between microplastic and natural

particulate dynamics in non-experimental situations (Vincent and Hoellein 2021). Collecting data that provide evidence for patterns of microplastic deposition and transport could allow scientists to harness hydrodynamic models initially created for natural particles to estimate microplastic flux and retention in riverine systems (Besseling et al. 2017). We must quantify these metrics reliably to define practical solutions to the global plastic pollution issue (Nizzetto et al. 2016).

This study aims to address the knowledge gap of microplastic distribution in rural riverine systems by quantifying abundance and composition in the Lower Flint River watershed in southwestern Georgia. The Lower Flint provides an ideal setting to investigate gaps in knowledge about the relationship between microplastic pollution and land cover, and to determine how certain physicochemical parameters relate to microplastic dynamics. I predicted that instream microplastic abundance would positively correlate with urban and agricultural land use in the Lower Flint watershed (McNeish et al. 2018). I also predicted that plastic concentrations would positively relate to measures of naturally occurring particles (Hoellein et al. 2019).

CHAPTER 2

METHODS

Data Collection

Study Area

I conducted longitudinal microplastics and water chemistry sampling at 16 sites on the mainstem and major tributaries of the Lower Flint River in southwestern Georgia (Figure 1). Additionally, I sampled directly below the Jim Woodruff Dam at the start of the Apalachicola River and at two additional tributaries that supply water to Lake Seminole (i.e., Spring Creek and the Chattahoochee River). I used established stations of a long-term water quality network, most of which had a corresponding United States Geological Survey (USGS) continuous stream flow monitoring station (Table 1). The mainstem Flint, Chattahoochee, and Spring Creek have urban areas and wastewater treatment plants, while Ichawaynochaway and Chickasawhatchee Creeks are dominated by agricultural land cover.

Spatial Data

I obtained Digital Elevation Models (DEMs) and land cover of the study area from the USGS 3D Elevation Program (3DEP) (USGS 2022) and the National Land Cover Database (NLCD) (USGS 2021), respectively. I delineated subwatersheds and recorded drainage areas for each sampling site using DEMs and ArcGIS Pro 2.9.2. I extracted 2019 NLCD data by individual subwatershed to estimate the basin land cover composition upstream of each stream sampling site. Land cover was categorized into Urban, Agricultural, and Forested. The Urban

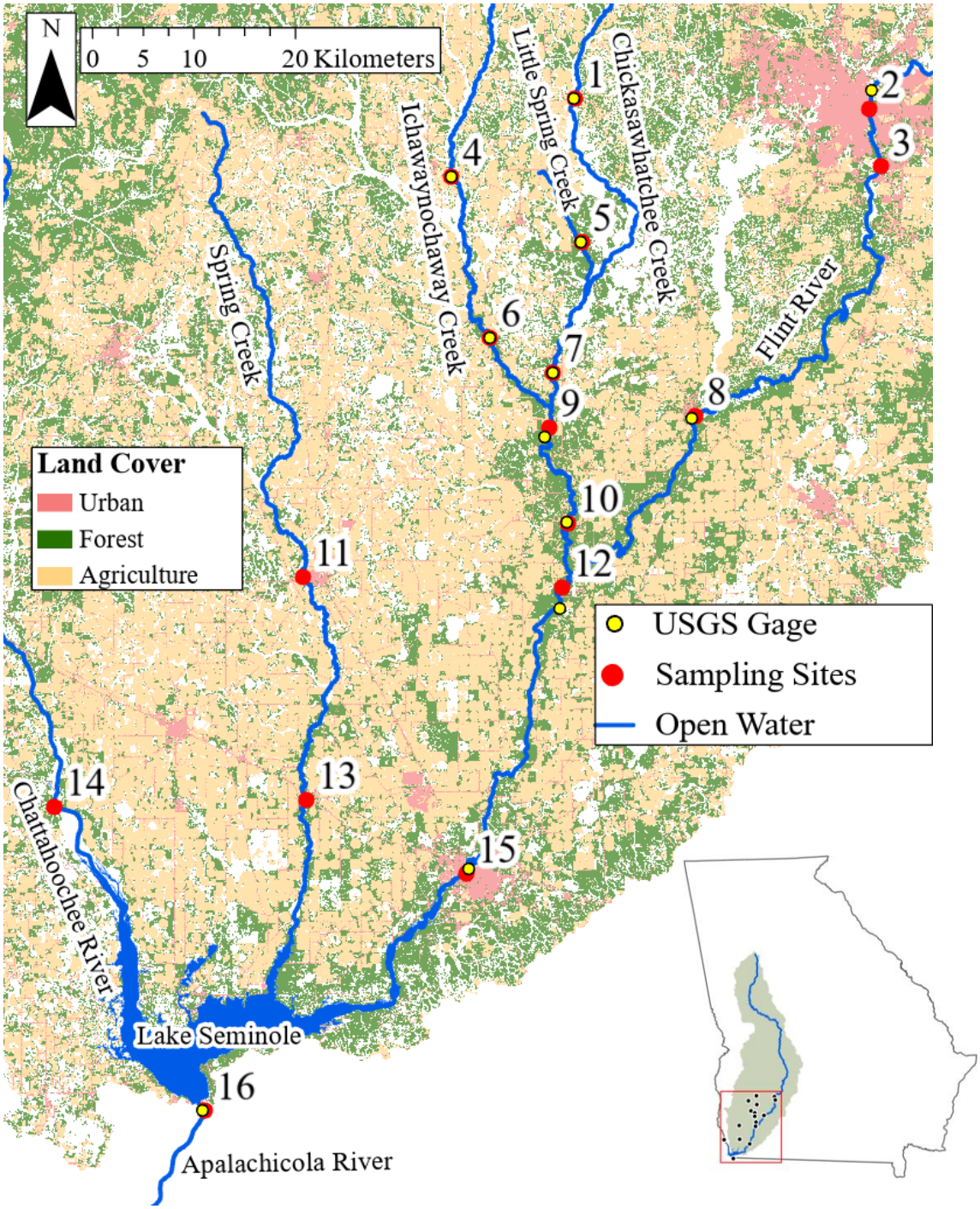

Figure 1. Map of the stream sampling sites (red dots), USGS gages (yellow dots), and land cover in southwestern Georgia, USA. Urban areas are shown in pink, forested areas in green, and agricultural land in yellow. Blue indicates major streams, rivers, and lakes.

Table 1. Summary of sampling site information. Stream sites are categorized into headwaters (H), midreaches (M), and rivers (R). Land cover types are forested (F), agricultural (A), and urban (U).

#	Stream Size	USGS Gage #	Latitude	Longitude	Drainage Area (km^2)	Land Cover (%) F	A	U
1	M	2354350	31.59350	-84.45290	303.93	25	44	6
2	R	2352500	31.57839	-84.14710	13,690.61	43	25	9
3	H	-	31.52630	-84.13670	18.61	13	59	16
4	M	2353265	31.52700	-84.58270	771.89	34	40	4
5	H	2354475	31.46570	-84.44930	37.35	27	42	3
6	M	2353500	31.38290	-84.54640	1,644.12	32	39	4
7	M	2354500	31.35070	-84.48259	808.41	28	30	4
8	R	2353000	31.30900	-84.33529	14,930.25	42	25	10
9	M	2354800	31.30170	-84.48690	2,568.49	31	37	4
10	M	2355350	31.21660	-84.47000	2,758.31	31	37	4
11	M	-	31.17390	-84.74490	733.07	19	44	5
12	R	2355662	31.15909	-84.47789	17,961.89	40	28	9
13	M	-	30.97529	-84.74559	1,530.56	18	51	5
14	R	-	30.97380	-85.00579	21,997.87	55	12	16
15	R	2356000	30.90670	-84.58260	19,312.62	40	29	8
16	R	2358000	30.70079	-84.85729	44,532.27	46	22	12

categories included "Developed, Open Space," "Developed, Low Intensity," "Developed, Medium Intensity," and "Developed, High Intensity." The agricultural category included "Cultivated Crops" and "Hay/Pasture." The forested category included "Deciduous Forest," "Evergreen Forest," and "Mixed Forest." The remaining NLCD classifications were combined as "Other" and excluded from the statistical analysis. Sampled streams were categorized by Strahler Stream Order into Headwaters (1-3), Midreaches (4-6), and Rivers (>6). Discharge was recorded for the corresponding USGS streamflow station from the USGS Current Conditions website using the measurement from the nearest 15-minute increment to the time of sample collection.

Sample Collection

Four water samples for microplastic analysis were collected in pre-washed and DI-rinsed 1-L amber Nalgene® bottles. Surface water samples were collected by submerging the bottle under the surface in a well-mixed area and then removing the cap until it filled with water. The bottle was held facing upstream, with the cap alongside, but below the mouth to avoid contamination. The cap was replaced while underwater to prevent contamination from the atmosphere. Microplastic water samples were stored in the lab at room temperature until processed.

Three water chemistry samples were collected directly below the water surface in acid-washed and DI-rinsed 1-L clear Nalgene® bottles. Bottles were rinsed three times with sample water before being filled. Water chemistry samples were put on ice and returned to the lab, where they were stored between 2-4 °C until processed. Conductivity, pH, and water temperature were measured using a Hydrolab Quanta Sonde (Hach Laboratories) or a Pocket Pro+ Multi 2 Tester (Hach Laboratories) when the Hydrolab was unavailable.

Laboratory Processing

Lab Preparation

All microplastic samples were processed in a designated lab where only individuals working on microplastics were permitted to enter. All technicians wore bright yellow cotton T-shirts and pants to render contamination from clothing easily identifiable, given that bright yellow fibers were rare in the field samples. The yellow clothing was worn during all fieldwork and laboratory sample processing. Lab surfaces were cleaned daily before any processing began to minimize contamination.

Microplastics Processing

Samples were shaken and poured through an 8-cm diameter, 25-µm sieve into an 8-cm diameter graduated cylinder. Beforehand, the sieve and graduated cylinder were washed and rinsed with 0.45-µm filtered DI water. The volume of the water sample was recorded. The sample bottle, cap, and sides of the sieve were rinsed three times each with filtered DI water through the sieve. Next, the contents of the sieve were rinsed with filtered DI water into a pre-washed and rinsed 4-oz. specimen cup. The sieve was rinsed with filtered DI water to remove any adhered material before processing the next sample. The sieve was washed and rinsed with filtered DI water between each set of four replicates. Thirty percent H_2O_2 was vacuum filtered through a cellulose acetate filter (Whatman™ ME 25/21 ST 0.45-µm gridded filter, 47 mm). Subsequently, 30 mL of 30% H_2O_2 was added to each specimen cup to digest non-plastic organic material (Wiggin & Holland, 2019). Sample cups were placed in a drying oven at 45 °C overnight (approximately 16 hours).

Following digestion, I used vacuum filtration to transfer the particulate contents of the specimen cups onto filters. Two of the four replicates for each sampling event were filtered onto

cellulose acetate filters, while the remaining two were filtered onto polycarbonate membrane filters (Isopore™ 0.8-µm PC Membrane, 47 mm). Before filtering, a chemically resistant marker was used to draw two intersecting lines on each filter to divide the filter into four equal quadrants. Next, samples were swirled and poured into the filter funnel, and specimen cups, lids, and the filter funnel were rinsed three times with filtered DI water. Between uses, the filter apparatus was covered with aluminum foil to avoid atmospheric contamination (Rochman et al. 2019). Cellulose acetate filters were stored in individual 51-mm aluminum weigh boats and covered with aluminum foil. Polycarbonate filters were stored in individual 47-mm petri slides for subsequent Nile Red staining.

The filters were examined under a dissection microscope at 25x-50x magnification (McNeish et al. 2018). Each quadrant of the filter was visually inspected in a clockwise direction, and microplastic particles were categorized and quantified. Particles were morphologically categorized as fibers, fiber bundles, foam, film, fragments, or pellets, and their color was recorded (McNeish et al. 2018, Rochman et al. 2019). If bright yellow fibers were detected, they were recorded but excluded from the final counts. Each filter was checked a second time by a different researcher or the same researcher at least two weeks after the initial count (McNeish et al. 2018). First and second counts that differed by more than four particles were counted a third time. If there was doubt that a particle was composed of plastic, it was subjected to the hot needle test (de Witte et al. 2014, Devriese et al. 2015). If the particle melted, it was considered plastic. If it singed, the particle was considered natural.

Polycarbonate filters were stained with 0.8-µm filtered Nile Red to detect fragments that were too small to be detected with standard visual identification (Maes et al. 2017, Wiggin and Holland 2019, Primpke et al. 2020). First, filters were placed in disposable filtration cups with

rinsed forceps. Next, 5 mL of Nile Red solution (10 µg/mL) was added. The solution was created with 99 mL of n-hexane and 1 mL of Nile Red stock solution. To make the 1 mg/mL stock solution, 10 mg of Nile Red was combined with 10 mL of acetone. The filtration cups were incubated in the staining solution in the dark for 30 minutes at room temperature. Next, the solution was removed via vacuum filtration, and each filter was rinsed with 5 mL of n-hexane three times. Filters were returned to their petri slides and covered with aluminum foil to avoid light exposure. Once dry, the filters underwent another round of visual inspection at 25-50x magnification under a microscope with light at a 455 nm wavelength. Fluorescent particles were considered plastic and categorized as fibers, fiber bundles, foam, film, fragments, or pellets. The counts of Nile Red stained filters were not included in final counts or statistical analyses.

Water Chemistry Processing

Water quality samples were vacuum filtered through a previously ashed and weighed 0.7-µm glass fiber filter. Sample aliquots were stored below 0 °C (NO_3-N and PO_4-P) or between 0-5 °C (DOC and NH_4-N). Filters were dried at 45 °C for 24 hours and weighed. Then, they were ashed (550 °C, 1 hour) and weighed again to calculate the dry mass (DM) and ash-free dry mass (AFDM). The concentrations of fine particulate organic matter (FPOM) and total suspended solids (TSS) were calculated from DM and AFDM. A Lachat QuickChem 8500 series two flow injection analyzer was used to measure NO_3-N (Lachat Method 10-107-04-1-B, 10-107-06-1-G), PO_4-P (Lachat Method 10-115-001-B), and NH_4-N (Lachat Method 10-107-06-1-G). Dissolved organic carbon (DOC), total dissolved carbon (TC), and dissolved inorganic carbon (DIC) were measured using a Shimadzu TOC-V total organic carbon analyzer.

Contamination Control

Four microplastic field blanks were taken each sampling day to account for contamination (Miller et al. 2021). The bottles were prepared identically to the field sample bottles and were taken on the sampling trip. The bottles were never opened, but the caps were twisted once to loosen and then retightened to mimic the bottle's opening. These blanks were then run through the entire microplastic analysis process. The average contamination per sampling day was calculated and then subtracted from total microplastic counts by morphology. Final counts were not corrected for particle color. The mean (± SD) contamination of blank samples was 1.85 ± 0.02 fibers and 1.59 ± 0.02 fragments per sample; therefore, two fibers and fragments were subtracted from each filter to account for contamination prior to statistical analyses. Three water chemistry field blanks were taken on each sampling day. Acid-washed, 1-L clear Nalgene® bottles were filled with DI water and brought on the sampling trip. The blanks were run through each nutrient and carbon analysis process. The average blank measurement per sampling day was taken and subtracted from the corresponding field collection day sample measurements. Three blank filters were used per sampling day for AFDM measurements. The average DM and AFDM per day were subtracted from sample measurements from the corresponding collection day.

Statistical Analysis

All statistical analyses were conducted using R version 4.0.4 (R Core Team 2021). Principal component analysis (PCA) was used as an exploratory analysis to investigate patterns in water chemistry, watershed features, and microplastic concentration and inform subsequent analyses (pcrcomp(), stats package; R Core Team 2021). Water chemistry data were collected as part of the sampling activities of a long-term water quality monitoring network with a previously

established sampling scheme and sites. For this reason, not all water quality measurements were taken at each sampling event, resulting in gaps in the data. The data were subset into variables of interest, and gaps were removed (na.omit(); R Core Team 2021). The resulting PCA included data collected from 15 sites on 22 sampling days.

Generalized linear mixed models (GLMMs) were conducted based on the PCA results to assess whether water chemistry variables or watershed features of interest explained instream microplastic concentration (glmmTMB(), glmmTMB package; Brooks et al. 2017). These statistical methods were modeled after those described by Hall et al. (2018), Nix et al. (2018), and Hou et al. (2021). Data gaps were removed before analysis, resulting in GLMMs generated from data collected at 12 sites on 21 sampling days. I used model selection (model.sel(), MuMIn package; Barton 2020) and Akaike's Information Criterion corrected for sample size (AIC_c) to identify the best-fitting statistical distribution for microplastic concentration (i.e., Gaussian, Poisson, negative binomial [NB], zero-inflated Poisson [ZIP], or zero-inflated negative binomial [ZINB]). Subsequently, the data were analyzed using the top-ranked negative binomial distribution (Table 2).

Univariate models were built for each explanatory variable as the fixed effect, with microplastic concentration as the response variable and site and sampling date as random effects (Table 3). Explanatory variables were assessed for correlation (rcorr(), Hmisc package; Harrell & Dupont 2021) and were considered correlated if they had an $r \geq 0.3$ (Appendix 1, Table 1). Bivariate GLMMs were built using all possible combinations of variables, excluding correlated ones. Site and sampling day were used as random effects. I conducted model selection to determine the best-fitting univariate, bivariate, and overall models by ranking them by AIC_c and model weights (w_i). Models were considered competing if the difference between their AIC_c and

the AIC_c of the top model (ΔAIC_c) was < 2. Using the best fitting models based on model selection, I created estimates of microplastic concentration based on significant predictors using back-transformed data (emmeans(), emmeans package; Lenth 2021). An additional GLMM was built to assess the impact of sampling site on microplastic concentration. The model included microplastic concentration as the response variable, sampling site as the fixed effect, and sampling day as a random effect. ANOVA Type III deviance models were used to determine if microplastic concentration varied across sampling sites, streams, and stream sizes (Anova(), car package; Fox & Weisberg 2019). The relative abundance of microplastic morphology was calculated for each sampling site, and a Chi Square Test of Independence (chisq.test(), stats package, R Core Team 2021) was used to examine if there was a significant association between relative abundance by morphology and site (McNeish et al. 2018).

Table 2: Akaike's information criterion corrected values for sample sizes (AICc) for the statistical distribution of microplastic concentration in the GLMM data subset. Distributions tested included the negative binomial (NB), zero-inflated negative binomial (ZINB), zero-inflated Poisson (ZIP), Poisson, and Gaussian.

Distribution	**AIC_c**	w_i
NB	750.79	0.7097
ZINB	752.58	0.2903
ZIP	814.30	< 0.0001
Poisson	955.04	< 0.0001
Gaussian	987.87	< 0.0001

Table 3. Physicochemical parameters and watershed features used as explanatory variables with corresponding abbreviations and units.

Explanatory Variable	**Abbreviation**	**Units**
Physicochemical parameters		
Total suspended solids	TSS	mg/L
Fine particulate organic matter	FPOM	mg/L
Total dissolved carbon	TC	mg/L
Dissolved organic carbon	DOC	mg/L
Dissolved inorganic carbon	DIC	mg/L
Ammonium	NH_4	ug/L
Nitrate	NO_3	ug/L
Soluble reactive phosphorous	SRP	ug/L
Conductivity	-	mS/cm
pH	-	-
Water temperature	-	°C
Watershed features		
Discharge	-	m^3/s
Drainage area	-	km^2
Stream	-	-
Stream order	-	-
Stream size	-	-
Percent urban	-	%
Percent forest	-	%
Percent agriculture	-	%

CHAPTER 3

RESULTS

Microplastic Abundance

Microplastics were detected at all sampling sites and were observed in 59% of 352 samples. The mean (± SD) microplastic concentration (particles/L) in the samples was 1.64 ± 2.17 (Table 4). The most abundant particle morphology was fragments (n = 291 particles, 49%), followed by fibers (n = 240 particles, 40%), fiber bundles (n = 33 particles, 6%), film (n = 15 particles, 3%), foam (n = 9 particles, 1%), and pellets (n = 9 particles, 1%) (Figure 2). The relative abundance of particle morphologies varied significantly with sampling site ($\chi^2 = 968.33$, df = 95, $P < 0.001$). In the 189 samples stained with Nile Red, 1,087 fragments were detected, for an average of 10.29 ± 22.65 fragments per sample.

Table 4. Morphology composition and average concentrations of all microplastic particles detected.

Morphology	Count	%	Average Concentration (particles/L) ± SD
Fragment	291	49	0.77 ± 1.56
Fiber	240	40	0.63 ± 1.19
Fiber Bundle	33	6	0.09 ± 0.28
Film	15	3	0.04 ± 0.21
Foam	9	1	0.02 ± 0.14
Pellet	9	1	0.02 ± 0.16
Total	597		1.64 ± 2.17

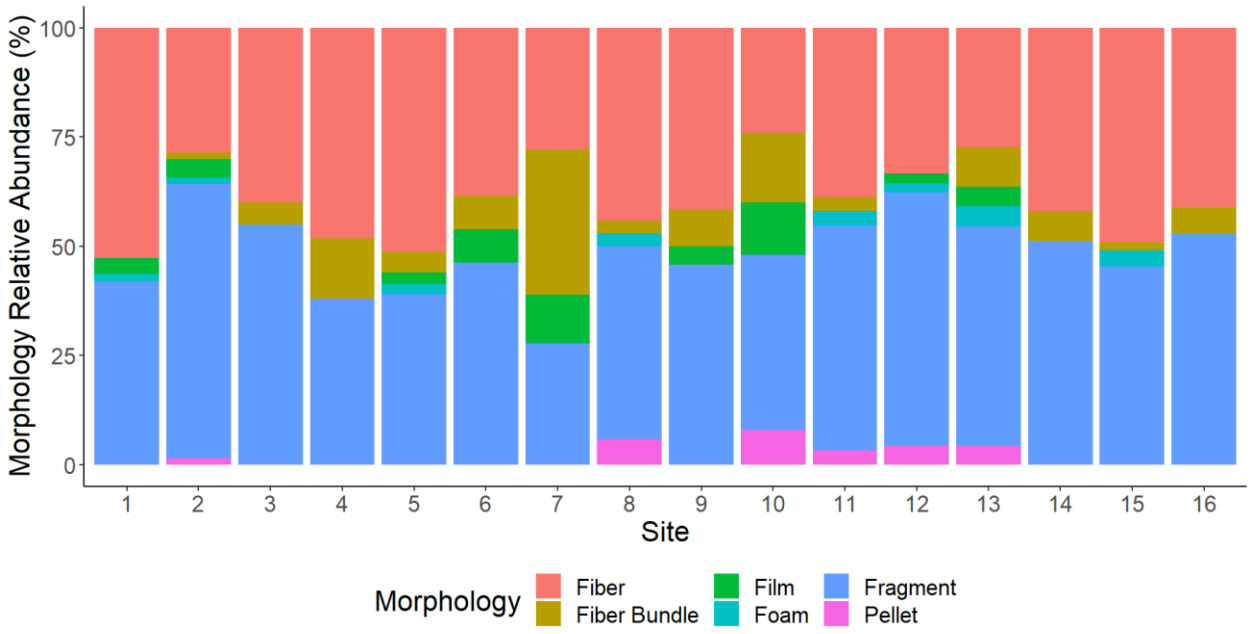

Figure 2. Percent abundance by particle morphology for each sampling site. The data presented represent the proportion of plastics collected from the sum of all the plastics collected from each sampling date at each sampling site.

Water Chemistry and Land Use

I focused on two dimensions of the PCA, principal components (PC) 1 and 3, which explained 39.9% and 11.6% of the variation, respectively (Table 5, Figure 3). I selected these components because the factor loadings of PC1 were strongly related to land use, and PC3 was associated with measures of particles, which were relationships of interest (Table 5). Sampling events tended to group by stream size, with rivers trending with higher measures of microplastics, fine organic particles, and phosphorous (i.e., SRP). Therefore, these relationships were explored in the subsequent GLMMs. Although PC1 represents a land use gradient, no clear land use patterns were related to microplastic concentration or stream size.

Table 5. Factor loadings of Principal Component (PC) 1-3.

	PC1	PC2	PC3
Microplastic	-0.1361	-0.2027	0.4784
FPOM	-0.1421	0.00127	0.20382
DOC	0.27346	0.42082	0.03052
DIC	0.36983	-0.2992	-0.2773
NH4	-0.1658	0.21672	-0.5268
SRP	-0.2414	-0.2918	0.35298
NO3	0.14068	-0.6082	-0.0475
Conductivity	0.32311	-0.3889	-0.2867
% Urban	-0.4066	-0.1195	-0.2926
% Agriculture	0.41838	0.10664	0.24011
% Forest	-0.4465	-0.1158	-0.1479

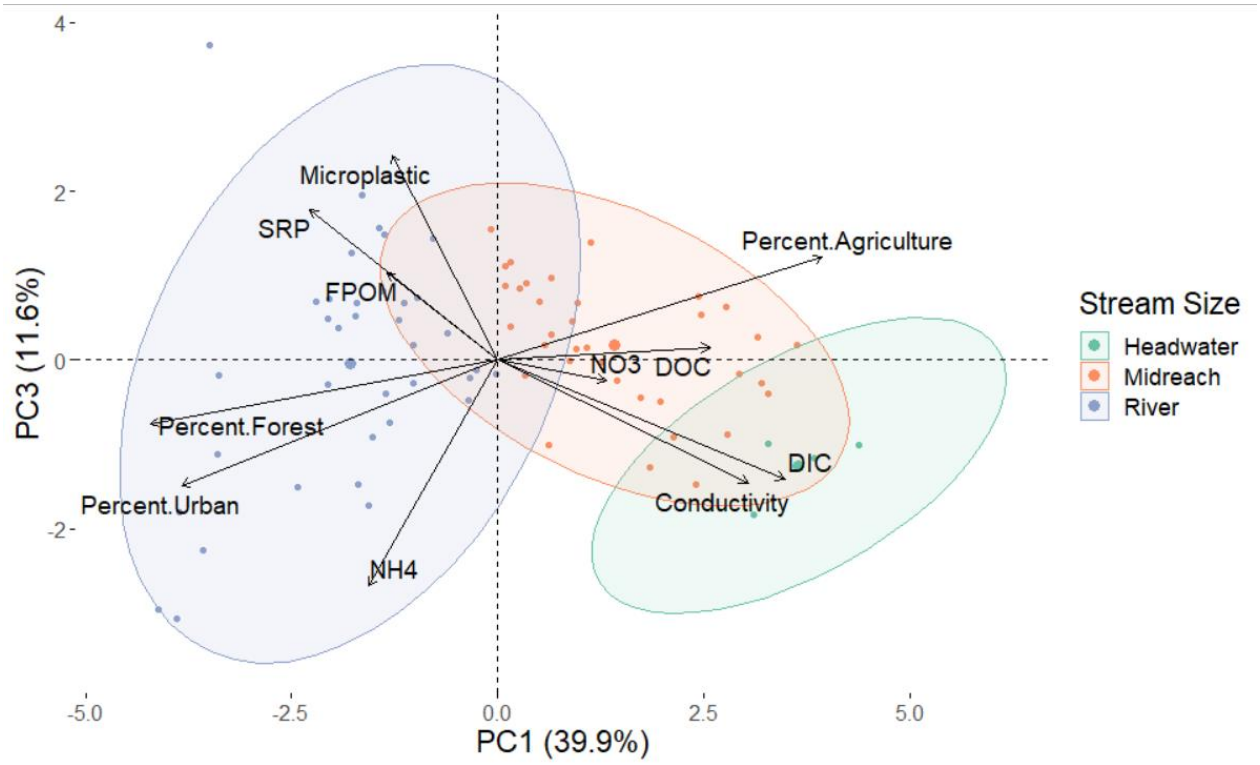

Figure 3. Projection of sampling events (dots) on the plane defined by PC1 and PC3. Arrows represent the direction and weight of vectors that demonstrate how water chemistry and land use variables explain variation. Ellipses (level = 0.95) and dot color indicate the stream size of the sampling site (green = headwaters, orange = midreaches, purple = rivers).

The headwater sites, which were primarily groundwater-fed, trended with DIC and conductivity, an expected pattern because these measures are indicative of groundwater influence in this region.

The best-fitting GLMM included SRP as the single fixed effect (Table 6). As the strongest predictor for microplastic concentration, SRP was included in all nine competing models and contributed to over 88% of the competing model weight. SRP was a significant positive coefficient for instream microplastic concentration (Table 7, Figure 4). Similar to patterns in the PCA, I found no significant relationship between land cover type (urban, agricultural, forested) and microplastic concentration ($p = 0.157$, $p = 0.941$, $p = 0.881$; respectively). Furthermore, sampling site did not explain microplastic concentration ($\chi^2 = 17.86$, $df = 11$, $P = 0.085$), nor did stream ($\chi^2 = 3.06$, $df = 4$, $P = 0.548$) (Figure 5). In contrast with my PCA results, stream size was not a significant explanatory variable for microplastic concentration ($\chi^2 = 1.69$, $df = 2$, $P = 0.429$) (Figure 5).

Contamination Control

Field controls contained a mean (± SD) contamination of 0.58 ± 1.21 microplastic particles per sample. Fibers were the dominant particle morphology found in the field control samples, with an average of 1.85 ± 0.02 particles/sample. There was an average contamination of 1.59 ± 0.02 fragments, 0.05 ± 0 fiber bundles, and 0.02 ± 0 film particles/sample. I detected no foam or pellets in the field controls.

Table 6. Model selection results evaluating the best and competing models for instream microplastic concentration as predicted by water chemistry and watershed features. Null models were included as a reference regardless of if they were competing models. LL is the log-link ratio; AIC_c is Akaike's information criterion corrected for sample sizes; ΔAIC_c is the difference from the best model; w_i is the AIC_c weight.

Model	*df*	LL	AICc	ΔAICc	w_i
SRP	5	-353.48	717.25	0	0.1665
SRP + FPOM	6	-352.75	717.91	0.66	0.1198
SRP + NO_3	6	-353.01	718.44	1.19	0.0919
SRP + Conductivity	6	-353.10	718.62	1.37	0.0840
SRP + TSS	6	-353.18	718.76	1.51	0.0781
SRP + NH_4	6	-353.22	718.84	1.59	0.0750
SRP + pH	6	-353.25	718.91	1.67	0.0724
SRP + Temperature	6	-353.32	719.06	1.81	0.0674
SRP + DIC	6	-353.39	719.19	1.94	0.0630
SRP + Drainage Area	6	-353.41	719.22	1.97	0.0620
Null (intercept with random effects)	4	-357.30	722.80	5.55	0.0104

Table 7. Model coefficients, statistical results, and 95% confidence intervals for the best-fitting model evaluating the effects of soluble reactive phosphorous on instream microplastic concentration.

					95% CI	
Coefficient	Estimate	SE	Z	*P*	Lower	Upper
Intercept	-0.3466	0.3061	-1.132	0.2575	-0.947	0.253
SRP	0.0758	0.0276	2.749	0.0060	0.022	0.130

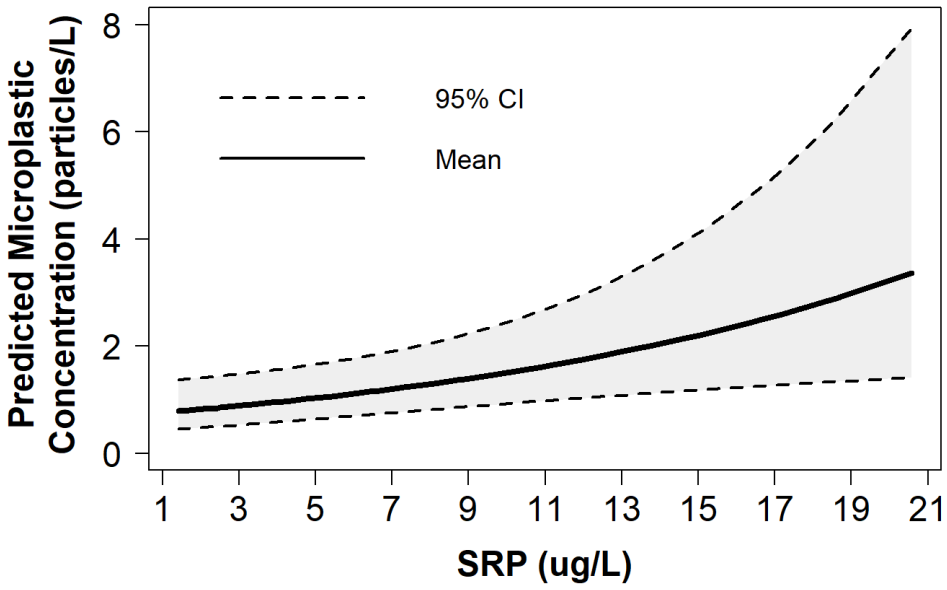

Figure 4. Microplastic concentration as predicted by soluble reactive phosphorus (SRP). Estimations were generated using the best-fitting GLMM (Table 6).

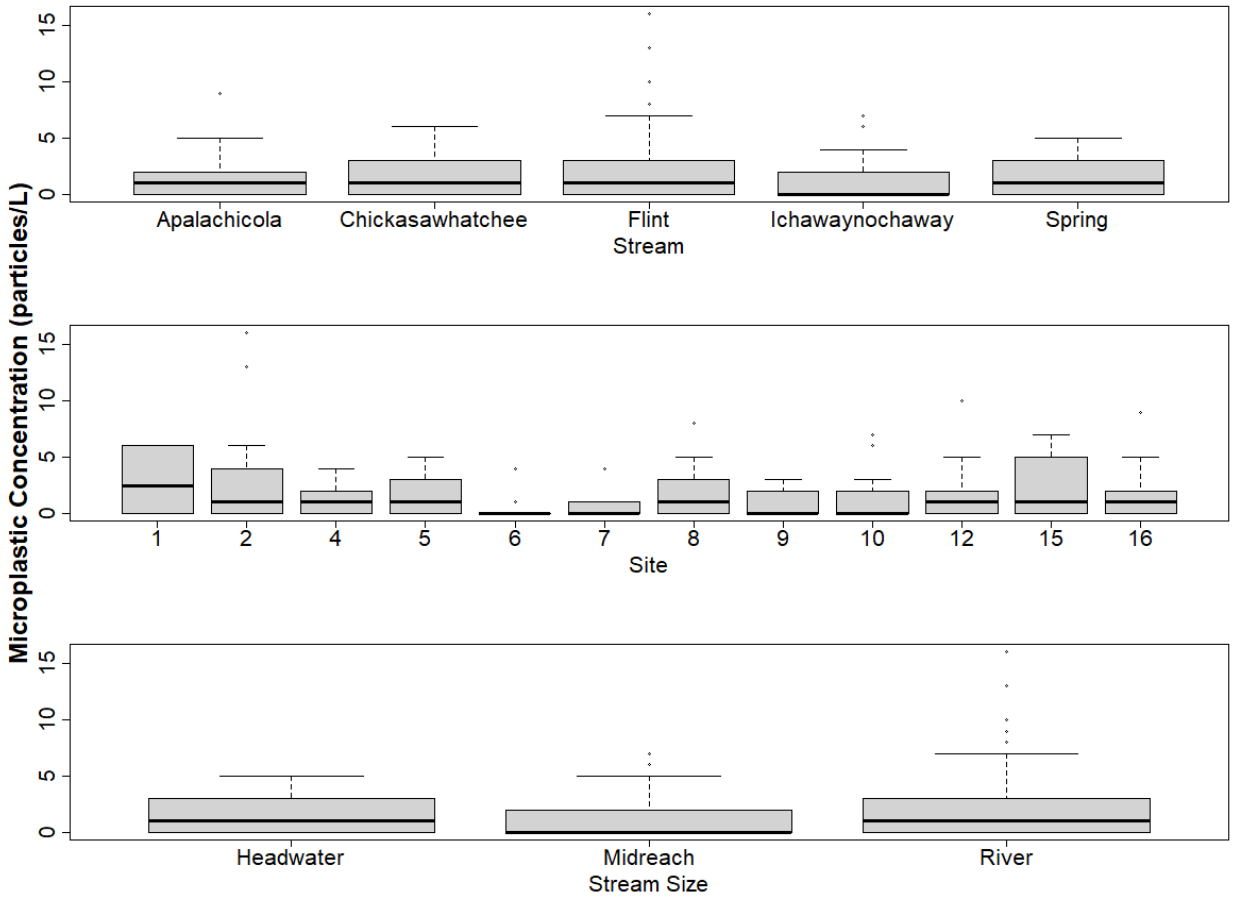

Figure 5. Boxplots of the average microplastic concentrations among sampling sites, streams, and stream sizes.

CHAPTER 4

DISCUSSION

Investigating microplastic dynamics within watersheds is critical to understanding the "plastic cycle" and estimating plastic storage and fluxes through freshwater systems. The results of this study provide additional insights into the plastic contamination of large, rural watersheds and evaluate relationships between the physicochemical conditions of the water column and plastic dynamics in river networks. By increasing our knowledge of microplastic dynamics in freshwater, we can better estimate global plastic budgets and inform strategies to reduce plastic emissions.

Effective management of emerging contaminants, such as microplastic, must occur at the watershed scale to account for point and non-point sources of contamination associated with variable land use. This is particularly true in agricultural watersheds, where non-point sources contribute substantially to surface water pollution. My research found that microplastic pollution is pervasive in the Lower Flint River basin's surface waters, as I could consistently detect contamination in surface waters despite the comparatively low human population density. The average concentration of microplastic I detected throughout the study area of 1.6 particles/L was similar to concentrations found in other studies conducted in rural settings (e.g., Chen et al., 2021; Talbot et al., 2022). I also found that the morphological composition of microplastic contamination depended on the sampling site, suggesting that local drivers and sources affected concentrations of particles. However, the sampling site, stream, and stream size did not predict microplastic concentrations, despite the large size of the study area.

An essential aspect of generalizing watershed-level plastic budgets is understanding how land cover relates to instream microplastic dynamics. Research has documented patterns in plastic contamination that were related to land use. For example, McNeish et al. (2018) found that human-dominated watersheds had elevated instream concentrations of microplastic compared to primarily forested watersheds due to both point- and non-point sources of plastic emissions. In contrast, I found no significant relationship between surface water microplastic concentration and the proportion of urban, agricultural, and forested land cover in the watershed. The results from my work could be attributed to the relatively short time frame of the study or the large drainage areas considered within the explanatory variables related to land use. To investigate patterns at a more local spatial scale, future work should consider taking a more nuanced approach to land use by constricting watershed sizes and integrating additional potential sources of plastic inputs, including boat ramps or road crossings, into the analyses.

Weather and climate patterns that influence stream discharge may also influence patterns in plastic dynamics (Barrows et al. 2018, Piñon-Colin et al. 2020). Barrows et al. (2018) found that discharge was negatively correlated with instream microplastic concentration in a mixed land-use watershed, suggesting that high flows diluted microplastic concentrations. Alternatively, results from Piñon-Colin et al. (2020) demonstrated that microplastic concentrations were positively associated with rainfall events in an urban setting, suggesting runoff-driven microplastic contamination. The sampling period of this study (June to November of 2021) was abnormally wet, and discharge within the Lower Flint was often above normal seasonal levels. Hence, I was unable to compare microplastic abundance during high- and low-flow scenarios. In the Lower Flint River basin, agriculture is typically concentrated in the uplands, away from direct runoff. Mature riparian forests may act as water quality filters,

mitigating plastic pollution entering the stream through overland flow. Notably, the study area is characterized by low surface water drainage density, with base flows in the karst landscape largely attributable to groundwater discharge. In this scenario, plastics may be retained in surface soils rather than transported through surface runoff. More empirical evidence is needed to understand the impacts of precipitation and runoff on microplastic concentrations in agriculturally dominated watersheds. Future work should conduct event-driven sampling over flow pulses to explore the hydrologic impacts of microplastic contamination in agriculturally dominated watersheds.

Relationships between discharge and plastic concentrations are essential to predict the contribution of individual watersheds to the plastic load entering lacustrine and marine environments. By coupling microplastic concentration estimates and average monthly discharge in dominant watersheds of the Lower Flint (readNWISdv, dataRetrieval package; de Cicco et al. 2022), I estimated microplastic flux in billions of microplastic particles per day entering and exiting Lake Seminole in southwestern Georgia (Appendix 1, Tables 3 & 4). Though there are limitations associated with estimates made over such a relatively short period with small volumes of water, on average, approximately 90.9 billion microplastic particles per day entered the reservoir via the three main branches (i.e., the Chattahoochee and Flint Rivers and Spring Creek) and 82.6 billion particles per day leave the dam and enter the Apalachicola River, traveling to the Gulf of Mexico. These estimates highlight the potential storage rates of microplastic pollution in reservoirs (~8.3 billion particles per day) and that billions of plastic particles flow from the Flint downstream daily. Reservoirs have been found to play an important role in removing and sequestering other human contaminants in river drainages (Webster et al.

2021), and it has been proposed that microplastics may also follow these deposition patterns (Hübner et al. 2020).

Soluble reactive phosphorous, or SRP, was the strongest predictor for microplastic abundance of all the explanatory variables tested. SRP is a measure of the bioavailable form of phosphorus in the water column, which readily absorbs to charged particles, such as clays, and often enters streams as sediment runoff. The relationship between microplastic and SRP in this study is notable because they both have major anthropogenic sources, including, but not limited to, industrial and municipal wastewater, urban and agricultural runoff, effluent from wastewater treatment plants, and atmospheric deposition (Jambeck et al. 2015, Allan et al. 2021). SRP is often measured in water quality monitoring programs; thus, if the relationship I documented between microplastic and SRP is ubiquitous in rural watersheds, the large body of knowledge related to temporal and spatial patterns in SRP dynamics could be harnessed in innovative ways to estimate microplastic fluxes through river systems with less labor-intensive methods.

Microplastic research has repeatedly demonstrated that plastic particles often behave similarly to natural particles in their movement through watersheds (Hoellein et al. 2019, Yan et al. 2021, Vincent and Hoellein 2021). As an allochthonous form of particulate carbon, microplastic is subject to the same chemical and physical processes that dictate the deposition and transport of natural particles in river systems. For natural particles, the concentration can be predicted from the rate of discharge on the rising limb of storm hydrographs (Golladay et al. 1987). The results of Chen et al. (2021) indicate that instream microplastic concentrations were positively associated with measures of suspended sediment concentrations, supporting the idea that microplastics follow natural particulate patterns. However, microplastics' physical and chemical properties differ from natural particles, which may cause them to behave differently in

the water column. Vincent & Hoellein (2021) found that FPOM and microplastics were retained together in a river system; however, due to differences in shape and densities, microplastics were more likely to become resuspended and were transported farther downstream. In this study, I found that when considered in univariate models, measures of natural suspended particles (FPOM and TSS) significantly explained microplastic concentrations in the Lower Flint (Appendix Table 2). Furthermore, the bivariate models that included SRP and either FPOM or TSS were among the top competing models, although the constituents were not significant predictors for microplastic concentration in the water column. Future work should further explore the relationship between microplastics and natural suspended particles relative to deposition, transport, and hydrologic drivers to comprehensively understand the similarities and differences between how they behave instream. This information will help identify possibilities and limitations of quantifying microplastic fluxes based on measures of natural particles.

Due to the microscopic size and ubiquity of microplastic pollution, analyzing environmental water samples for microplastics presents challenges related to contamination and identification (Miller et al. 2021). In this study, all microplastic counts were blank corrected by morphology, but not by color and size, potentially causing the final counts to underestimate particle concentrations. Furthermore, I found an average of 0.49 microplastic fragments per sample; however, the Nile Red stained filters had an average of 10.29 fragments per sample. The underestimation of microplastic fragments in final counts could be attributed to the fluorescence from Nile Red stained particles allowing the observer to detect smaller particles than they originally could from visual inspection only. All samples were collected at the water surface, and the remaining water column was not considered in this study. For this reason, overall

microplastic abundance may have been underestimated (Barrows et al. 2017), although I generally sampled shallow rivers in well-mixed areas.

The implications of this study suggest that microplastic contamination is ubiquitous throughout the globe, and this work demonstrated that microplastic pollution is also pervasive in agriculturally dominated rural watersheds. This research builds upon the findings of others to suggest that plastics may behave similarly to natural particles, and they appear to have a strong relationship with concentrations of bioavailable phosphorus in the water column. Though we can leverage our knowledge of the behavior of natural particles and existing hydrodynamic models that estimate transport, sedimentation, and resuspension to understand microplastic movement, more empirical studies are needed to investigate these relationships to elucidate the contribution of river networks on plastic transport and retention over broad spatial and temporal scales. Nizzetto et al. (2016) argues that it is impractical to clean up plastic pollution once it reaches the ocean; therefore, we must focus on terrestrial transport processes and managing our emissions into the natural environment to combat the global problem of plastic pollution. We can estimate global plastic budgets more reliably by developing a comprehensive understanding of plastic movement through freshwater systems. Consequently, this information will allow us to advise plastic pollution reduction strategies and shape global policy change.

REFERENCES

Allan, J. D., M. M. Castillo, and K. A. Capps. 2021. Stream Ecology: Structure and Function of Running Waters. Third edition. Springer Nature Switzerland AG.

Barrows, A. P. W., K. S. Christiansen, E. T. Bode, and T. J. Hoellein. 2018. A watershed-scale, citizen science approach to quantifying microplastic concentration in a mixed land-use river. Water Research 147:382–392.

Barrows, A. P. W., C. A. Neumann, M. L. Berger, and S. D. Shaw. 2017. Grab: Vs. neuston tow net: A microplastic sampling performance comparison and possible advances in the field. Analytical Methods 9:1446–1453.

Barton, K. 2020. MuMIn: Multi-Model Inference. R package version 1.43.17.

Besseling, E., J. T. K. Quik, M. Sun, and A. A. Koelmans. 2017. Fate of nano- and microplastic in freshwater systems: A modeling study. Environmental Pollution 220:540–548.

Borrelle, S. 2020. Predicted growth in plastic waste exceeds efforts to mitigate plastic pollution. Science 1518:1515–1518.

Brandes, E., M. Henseler, and P. Kreins. 2021. Identifying hot-spots for microplastic contamination in agricultural soils - A spatial modelling approach for Germany. Environmental Research Letters 16:104041.

Brooks, M. E., K. Kristensen, K. J. van Benthem, A. Magnusson, C. W. Berg, A. Nielsen, H. J. Skaug, M. Maechler, and B. M. Bolker. 2017. glmmTMB Balances Speed and Flexibility Among Packages for Zero-inflated Generalized Linear Mixed Modeling. The R Journal 9: 378-400.

Chen, H. L., C. N. Gibbins, S. B. Selvam, and K. N. Ting. 2021. Spatio-temporal variation of microplastic along a rural to urban transition in a tropical river. Environmental Pollution 289:117895.

De Witte, B., L. Devriese, K. Bekaert, S. Hoffman, G. Vandermeersch, K. Cooreman, and J. Robbens. 2014. Quality assessment of the blue mussel (Mytilus edulis): Comparison between commercial and wild types. Marine Pollution Bulletin 85:146–155.

Devriese, L. I., M. D. van der Meulen, T. Maes, K. Bekaert, I. Paul-Pont, L. Frère, J. Robbens, and A. D. Vethaak. 2015. Microplastic contamination in brown shrimp (Crangon crangon, Linnaeus 1758) from coastal waters of the Southern North Sea and Channel area. Marine Pollution Bulletin 98:179–187.

Eibes, P. M., and F. Gabel. 2022. Floating microplastic debris in a rural river in Germany: Distribution, types and potential sources and sinks. Science of the Total Environment 816:151641.

Fox, J., and S. Weisberg. 2019. An {R} Companion to Applied Regression, Third Edition. Thousand Oaks CA: Sage.

Geyer, R., J. R. Jambeck, and K. L. Law. 2017. Production, use, and fate of all plastics ever made. Science Advances 3:25-29.

Golladay, S. W., J. R. Webster, and E. F. Benfield. 1987. Changes in Stream Morphology and Storm Transport of Seston Following Watershed. Page Source: Journal of the North American Benthological Society 6:1-11.

Hall, L. K., R. T. Larsen, R. N. Knight, and B. R. McMillan. 2018. Feral horses influence both spatial and temporal patterns of water use by native ungulates in a semi-arid environment. Ecosphere 9:e02096.

Harrell Jr., F. E., and C. Dupont. 2021. Hmisc: Harrell Miscellaneous. R package version 4.5-0.

Hoellein, T. J., and C. M. Rochman. 2021. The “plastic cycle”: a watershed-scale model of plastic pools and fluxes. Frontiers in Ecology and the Environment 19:176-183.

Hoellein, T. J., A. J. Shogren, J. L. Tank, P. Risteca, and J. J. Kelly. 2019. Microplastic deposition velocity in streams follows patterns for naturally occurring allochthonous particles. Scientific Reports 9:1-11.

Hou, L., C. D. McMahan, R. E. McNeish, K. Munno, C. M. Rochman, and T. J. Hoellein. 2021. A fish tale: a century of museum specimens reveal increasing microplastic concentrations in freshwater fish. Ecological Applications 31:e02320.

Hübner, M. K., D. N. Michler-Kozma, and F. Gabel. 2020. Microplastic concentrations at the water surface are reduced by decreasing flow velocities caused by a reservoir. Fundamental and Applied Limnology 194:49–56.

Jambeck, J. R., R. Geyer, C. Wilcox, T. R. Siegler, M. Perryman, A. Andrady, R. Narayan, and K. L. Law. 2015. Plastic waste inputs from land into the ocean. Science 347:768–771.

Khatmullina, L., and I. Isachenko. 2017. Settling velocity of microplastic particles of regular shapes. Marine Pollution Bulletin 114:871–880.

Kumar, R., P. Sharma, A. Verma, P. K. Jha, P. Singh, P. K. Gupta, R. Chandra, and P. v. Vara Prasad. 2021. Effect of physical characteristics and hydrodynamic conditions on transport and deposition of microplastics in riverine ecosystem. Water 13:2710.

Lenth, R. V. 2021. emmeans: Estimated Marginal Means, aka Least-Squares Means. R package version 1.5.4.

Li, C., R. Busquets, and L. C. Campos. 2020. Assessment of microplastics in freshwater systems: A review. Science of the Total Environment 707:135578.

Maes, T., R. Jessop, N. Wellner, K. Haupt, and A. G. Mayes. 2017. A rapid-screening approach to detect and quantify microplastics based on fluorescent tagging with Nile Red. Scientific Reports 7:44501.

McCormick, A., T. J. Hoellein, S. A. Mason, J. Schluep, and J. J. Kelly. 2014. Microplastic is an abundant and distinct microbial habitat in an urban river. Environmental Science and Technology 48:11863–11871.

McNeish, R. E., L. H. Kim, H. A. Barrett, S. A. Mason, J. J. Kelly, and T. J. Hoellein. 2018. Microplastic in riverine fish is connected to species traits. Scientific Reports 8:11639.

Miller, E., M. Sedlak, D. Lin, C. Box, C. Holleman, C. M. Rochman, and R. Sutton. 2021. Recommended best practices for collecting, analyzing, and reporting microplastics in environmental media: Lessons learned from comprehensive monitoring of San Francisco Bay. Journal of Hazardous Materials 409:124770.

Nix, J. H., R. G. Howell, L. K. Hall, and B. R. McMillan. 2018. The influence of periodic increases of human activity on crepuscular and nocturnal mammals: Testing the weekend effect. Behavioural Processes 146:16–21.

Nizzetto, L., G. Bussi, M. N. Futter, D. Butterfield, and P. G. Whitehead. 2016. A theoretical assessment of microplastic transport in river catchments and their retention by soils and river sediments. Environmental Science: Processes and Impacts 18:1050–1059.

Piñon-Colin, T. de J., R. Rodriguez-Jimenez, E. Rogel-Hernandez, A. Alvarez-Andrade, and F. T. Wakida. 2020. Microplastics in stormwater runoff in a semiarid region, Tijuana, Mexico. Science of the Total Environment 704:135411.

Primpke, S., S. H. Christiansen, W. Cowger, H. de Frond, A. Deshpande, M. Fischer, E. B. Holland, M. Meyns, B. A. O'Donnell, B. E. Ossmann, M. Pittroff, G. Sarau, B. M.

Scholz-Böttcher, and K. J. Wiggin. 2020. Critical Assessment of Analytical Methods for the Harmonized and Cost-Efficient Analysis of Microplastics. Applied Spectroscopy 74:1012–1047.

R Core Team. 2021. R: A language and environment for statistical computing. R Foundation for Statistical Computing, Vienna, Austria.

Rehm, R., T. Zeyer, A. Schmidt, and P. Fiener. 2021. Soil erosion as transport pathway of microplastic from agriculture soils to aquatic ecosystems. Science of the Total Environment 795:148774.

Rillig, M. C. 2020. Microplastic in terrestrial ecosystems. Environmental Science and Technology 368:1430–1431.

Rochman, C. M., C. Brookson, J. Bikker, N. Djuric, A. Earn, K. Bucci, S. Athey, A. Huntington, H. McIlwraith, K. Munno, H. de Frond, A. Kolomijeca, L. Erdle, J. Grbic, M. Bayoumi, S. B. Borrelle, T. Wu, S. Santoro, L. M. Werbowski, X. Zhu, R. K. Giles, B. M. Hamilton, C. Thaysen, A. Kaura, N. Klasios, L. Ead, J. Kim, C. Sherlock, A. Ho, and C. Hung. 2019. Rethinking microplastics as a diverse contaminant suite. Environmental Toxicology and Chemistry 38:703-711.

Talbot, R., E. Granek, H. Chang, R. Wood, and S. Brander. 2022. Spatial and temporal variations of microplastic concentrations in Portland's freshwater ecosystems. Science of The Total Environment 833:155143.

U. S. Geological Survey. 2021. National Land Cover Database. https://www.usgs.gov/centers/eros/science/national-land-cover-database.

U. S. Geological Survey. 2022. 3D Elevation Program. https://www.usgs.gov/3d-elevation-program.

Vethaak, B. A. D., and J. Legler. 2021. Microplastics and Human Health. Science 371:672-674.

Vincent, A. E. S., and T. J. Hoellein. 2021. Distribution and transport of microplastic and fine particulate organic matter in urban streams. Ecological Applications 31:e02429.

Waldschläger, K., and H. Schüttrumpf. 2019. Erosion Behavior of Different Microplastic Particles in Comparison to Natural Sediments. Environmental Science and Technology 53:13219-13227.

Webster, B. C., M. N. Waters, and S. W. Golladay. 2021. Alterations to sediment nutrient deposition and transport along a six reservoir sequence. Science of the Total Environment 785:147246.

Wiggin, K. J., and E. B. Holland. 2019. Validation and application of cost and time effective methods for the detection of 3–500 µm sized microplastics in the urban marine and estuarine environments surrounding Long Beach, California. Marine Pollution Bulletin 143:152–162.

Wright, S. L., and F. J. Kelly. 2017. Plastic and Human Health: A Micro Issue? Environmental Science and Technology 51:6634–6647.

Yan, M., L. Wang, Y. Dai, H. Sun, and C. Liu. 2021. Behavior of Microplastics in Inland Waters: Aggregation, Settlement, and Transport. Bulletin of Environmental Contamination and Toxicology 107:700-709.

APPENDIX 1

Appendix Table 1. Correlation matrix of explanatory variables. Q is the rate of discharge in meters^3/second. Temp. is water temperature in °C. Cond. is conductivity in mS/cm. % Urban, Forest, and Ag indicate the percent of urban, forested, and agricultural land cover in the watershed, respectively.

	TSS	FPOM	DOC	TC	DIC	NH4	SRP	NO3	Q	Temp.	Cond.	pH	Area	% Urban	% Forest
TSS															
FPOM	0.83														
DOC	0.27	0.06													
TC	-0.28	-0.16	0.47												
DIC	-0.39	-0.20	0.23	0.96											
NH4	0.25	0.41	0.12	0.03	-0.01										
SRP	0.29	0.21	-0.26	-0.32	-0.28	-0.19									
NO3	-0.23	0.01	-0.40	0.34	0.47	-0.25	-0.02								
Q	0.36	0.27	-0.05	-0.27	-0.29	0.12	0.36	-0.16							
Temp.	-0.04	0.03	-0.02	-0.16	-0.17	0.22	0.02	-0.46	-0.05						
Cond.	-0.39	-0.17	0.14	0.87	0.91	-0.04	-0.11	0.50	-0.20	-0.15					
pH	-0.32	-0.05	-0.48	0.08	0.24	0.09	0.01	0.22	0.03	0.06	0.28				
Area	0.01	0.13	-0.42	-0.28	-0.19	0.09	0.29	-0.01	0.83	0.03	-0.08	0.33			
% Urban	0.09	0.15	-0.45	-0.42	-0.33	0.09	0.58	-0.12	0.76	0.07	-0.18	0.28	0.89		
% Forest	0.14	0.16	-0.53	-0.54	-0.44	-0.14	0.58	-0.04	0.70	0.03	-0.30	0.17	0.82	0.89	
% Ag	-0.06	-0.09	0.34	0.28	0.20	0.12	-0.56	0.13	-0.68	-0.04	0.08	-0.30	-0.80	-0.87	-0.90

Appendix Table 2. Model coefficients, statistical results, and 95% confidence intervals for the univariate models evaluating the effects of TSS and FPOM on instream microplastic concentration.

					95% CI	
Coefficient	Estimate	SE	Z	*P*	Lower	Upper
Intercept	-0.1401	0.2684	-0.522	0.602	-0.666	0.386
FPOM	0.2003	0.0861	2.326	0.020	0.032	0.369
Intercept	-0.1141	0.2774	-0.411	0.681	-0.658	0.430
TSS	0.0460	0.0213	2.164	0.030	0.004	0.088

Appendix Table 3. Estimated microplastic flux of inputs and output of Lake Seminole. The three inputs are Site 14 on the Chattahoochee River, Site 13 on Spring Creek, and Site 15 on the Flint River. Site 16 is the start of the Apalachicola River below the Jim Woodruff Dam and is considered the output. The USGS stations used for discharge are #02343801 for Site 14 and #02357000 for Site 13. The stations for Sites 15 and 16 are given in Table 1. MP is microplastic and BLD is billion liters per day. I did not estimate flux for the months and sites I did not detect any microplastics, shown by a dash (-).

Month	Site	Average MP Concentration (particles/L)	Average Monthly Discharge (BLD)	Flux (Billion MP/Day)
June	14	3.33 ± 1.59	18.04 ± 9.58	60.12
	13	2.12 ± 1.92	0.37 ± 0.23	0.79
	15	6.71 ± 0.92	12.83 ± 3.73	86.13
	16	1.85 ± 2.06	35.32 ± 9.83	65.41
July	14	-	26.83 ± 12.01	-
	13	0.31 ± 0.45	1.49 ± 0.34	0.46
	15	1.82 ± 2.02	17.06 ± 2.24	31.02
	16	-	51.38 ± 12.57	-
August	14	1.82 ± 1.31	27.63 ± 15.85	50.24
	13	0.69 ± 0.78	1.53 ± 0.00	1.06
	15	0.93 ± 0.95	17.42 ± 0.00	16.14
	16	0.69 ± 0.40	51.90 ± 0.02	35.60
September	14	0.93 ± 0.95	26.14 ± 7.09	24.20
	13	-	1.81 ± 0.88	-
	15	1.64 ± 1.97	18.05 ± 4.76	29.63
	16	4.02 ± 2.92	50.43 ± 11.40	202.72
October	14	3.19 ± 2.50	31.29 ± 29.88	99.83
	13	0.69 ± 0.77	1.04 ± 0.37	0.71
	15	2.50 ± 2.57	22.87 ± 12.23	57.17
	16	1.38 ± 0.81	62.28 ± 37.27	85.99
November	14	1.42 ± 1.45	17.87 ± 3.80	25.29
	13	1.87 ± 0.02	0.66 ± 0.26	1.24
	15	0.69 ± 0.41	12.56 ± 2.36	8.72
	16	0.72 ± 0.81	32.35 ± 2.30	23.18

Appendix Table 4. Average microplastic flux entering and exiting Lake Seminole from the three riverine arms into the reservoir. The three inputs are the Chattahoochee River, Spring Creek, and Flint River and the output is the Apalachicola River. The total average input flux is the sum of the average fluxes for Sites 13, 14, and 15. Output flux is the average flux of Site 16. MP/L is microplastic particles/liter.

Site	Average Input (Billions MP/L)	Average Output (Billions MP/L)
14	51.94	-
13	0.85	-
15	38.14	-
16	-	82.58
Total	90.92	82.58